Multivalued Solution and Viscosity Solutions of the Eikonal Equation

Jean-David Benamou

INRIA

INSTITUT NATIONAL DE RECHERCHE EN INFORMATIQUE ET EN AUTOMATIQUE

Multivalued solution and viscosity solutions of the Eikonal equation

Jean-David Benamou

N° 3281

Octobre 1997

THÈME 4

ISSN 0249-6399

Multivalued solution and viscosity solutions of the Eikonal equation

Jean-David Benamou

Thème 4 — Simulation et optimisation
de systèmes complexes
Projet Ondes

Rapport de recherche n ° 3281 — Octobre 1997 — pages

Abstract: Some contributions to the study and computation of the multivalued solution of the Eikonal equation

Key-words:

(Résumé : tsvp)

"Whether I live or die is immaterial. It is enough to know that there are people who commit time, money and energy to fight this one evil among so many others predominating worldwide. If they do not succeed today, they will succeed tomorrow. We must keep on striving to make the world a better place for all of mankind - each one contributing his bit, in his or her own way."

Ken Saro-Wiwa (May 1995).

Unité de recherche INRIA Rocquencourt
Domaine de Voluceau, Rocquencourt, BP 105, 78153 LE CHESNAY Cedex (France)
Téléphone : 01 39 63 55 11 - International : +33 1 39 63 55 11
Télécopie : (33) 01 39 63 53 30 - International : +33 1 39 63 53 30

Solution multivaluée et solutions de viscosité de léquation Eikonale

Résumé : Contributions à l'étude et au calcul des solutions multivaluees de l'équation Eikonale

Mots-clé : Hamilton-Jacobi, Calculus of Variation, Fermat Principle, Geometrical Optics, Geometrical Theory of Diffraction, Ray Tracing, Multi-Valued Travel Time Field, Viscosity Solution, Upwind Scheme, ENO scheme, High Frequency Asymptotic, Wave equation, eikonal equation, Hyperbolic Equation, Transport equation, Amplitudes

Contents

1 Introduction

In a previous paper [9] a method, called "Big Ray Tracing" (BRT) and based on ray tracing and "upwind" finite differencing (or Riemann solving) of the eikonal equation, was presented. It was designed to compute multi-valued travel time fields corresponding to high frequency

asymptotics of the wave equation. This multi-valued travel time field is also known as the geometric solution of the eikonal equation [17]. The computation of the geometric solution using direct solves of the eikonal equation (or methods other than "classical" ray tracing) is currently an active research topic. See [9] [4] [5] [6] [29] and their references on this subject and its applicative impact.

The idea of BRT was roughly to use the information on the geometric solution (in phase space) of the eikonal equation given by standard ray tracing to define local domains (in physical space) supporting different branches of the geometric solution. Then, except for "degenerate" situations corresponding to the presence of caustic points (a caustic can be defined simply as a locus where the rays of the geometrical optics have an envelope), the local "viscosity" solutions, computed using a suitable "upwind" finite difference scheme, was identified as the correct local minima for the optimal control problem (Fermat principle) corresponding the the Hamilton-Jacobi equation (eikonal equation).

This report has two separate part. The first part is twofold : First, we have a theoretical discussion in which we address the problem of these "degenerate" cases and propose a corrected BRT algorithm based on the geometrical theory of diffraction [21] [23]. The modified algorithm can handle reflection both on caustics and scaterring boundaries. Second, we detail the numerical implementation of the method. We also describe how amplitude computations could be added to this method. A numerical test problem is solved.

The second part presents a review of different methods for the same problem.

2 Classical Ray Tracing and BRT

In this section we review the problem of the multi-valued travel time computations and the mathematical background underlying BRT.

2.1 The geometric solution/Hamilton Jacobi equation

Travel (or arrival) times of optical, elastic or acoustic high frequency waves are classically computed using ray tracing [11]. Rays are "shot" from a source point in all directions or from a given surface in phase space (a plane wave for instance). Wavefronts (contour lines of the travel time) propagate along the rays. These paths (the rays) are obtained by solving a set of ordinary differential equations : the ray equations. Travel times along the rays are given by integrating the slowness index locally characterizing the medium. In the case of heterogeneous smooth slowness media, rays may cross and multiple travel times can occur at their intersection as associated wave fronts interact. This multi-valued solution is called the geometric solution.

The rays $y(t)$ are solution of the Hamiltonian system :

$$\begin{cases} \dfrac{dy}{dt} = pc(y)^2 \\ \dfrac{dp}{dt} = p^2 c(x) \nabla_x c(y) \end{cases} \tag{1}$$

also known as the ray equations. The velocity (strictly positive) is noted c and $1/c$ is the slowness. We assume throughout this paper that c is continuous up to its second derivatives. The system (1) must be supplemented with initial conditions. A popular way of computing the geometric solution associated to an isotropic source point x_0 is to solve (1) with initial conditions :

$$\begin{cases} y(0) = x_0 \\ p(0) = (cos(\theta), sin(\theta)) \end{cases} \tag{2}$$

where each θ in $[0, 2\pi[$ defines a ray. This is called ray tracing. Travel time along the ray is given by

$$\tau(y(t)) = \int_0^t \frac{1}{c(y(s))}\, ds \tag{3}$$

where s is the curvilinear abscissa.

There are at least two ways of (formally) deriving the equations of geometrical optics. We first start from the Fermat principle. It is usually formulated as a "minimum travel time" problem from a point A to a point B. The travel time is given as the infimum of the functional

$$J[y] = \int_A^B \frac{1}{c(y(s))}\, ds \tag{4}$$

over all the smooth (notion to be defined precisely) paths y going from A to B (we recall that c is the velocity, $1/c$ is the slowness and s is the curvilinear abscissa). This optimization problem can be set in the framework of the calculus of variation [33]. Different equivalent forms can be obtained for the Hamiltonian depending on time parameterization (which must not be confused with travel time) of the paths y. We take :

$$H(x, p) = \frac{1}{2}(p^2 c(x)^2 - 1) \tag{5}$$

where $x =\in \mathbb{R}^{2,3}$ and p is of the same dimension (p^2 is to be understood as the scalar product of p with itself). Then the Hamiltonian system characterizing stationary (or critical) paths is given by (1) and the travel time τ is a solution of the Hamilton-Jacobi equation :

$$H(x, \nabla\tau(x)) = 0. \tag{6}$$

We discuss the sense to be given to the solution of this equation in the next subsection.

Note that travel time is actually characterized by stationary paths and not by minima so that the above formulation of the Fermat principle is somewhat abusive. Stationary paths can be made of minima but also portions of minima separated by conjugate points. For y to realize a (possibly local) minimum of this problem, one must check that the ray does not go through a conjugate point before it reaches B ([33]). It means that the quadratic form associated to the second variation of the cost function (4) is non-negative. This degenerate case is discussed in [9] [25] where caustic points are identified as conjugate points. We come back on that point in section 3.

Another way to the eikonal equation is to assume that the solution u of the reduced wave equation

$$\Delta u + \omega^2 u = 0 \tag{7}$$

has the form of a particular ansatz

$$u(x) = e^{i\omega\tau(x)} \sum_{k=0}^{+\infty} \frac{A_k(x)}{(i\omega)^k} \tag{8}$$

where ω is the frequency, τ represents the phase of the solution and the sum of the series (A_k) the amplitude. We can replace u by this ansatz in the wave equation and expand this expression in powers of ω. Equating to 0 the terms corresponding to the first two powers of ω gives

$$\|\nabla_x \tau(x)\|^2 = \frac{1}{c(x)^2} \tag{9}$$

$$2\nabla_x \tau(x).\nabla_x A_0(x) + \Delta\tau(x) A_0(x) = 0 \tag{10}$$

known respectively as the eikonal (same as (6)) and transport equations. Their solutions are used in the ansatz (8) to give an approximate asymptotic (for large ω) solution of the wave equation. The ray equations can again be derived from (9). Details on this approach can be found in any physics monograph reviewing geometrical optics. It is well known that geometrical optics fails around caustics. It fails in the sense that near caustic points the amplitude given by (10) blows up. This is closely related to the notion of conjugate points. A modified theory called Geometrical Theory of Diffraction [20] [23] based on a different ansatz is uniformly valid around caustics. We review and use part of this theory in section 3.

Note finally that a rigorous mathematical derivation of this asymptotic model (based on a Wigner transform technique) can be found in [16].

2.2 Viscosity solutions and local minima

A voluminous literature is available on the relations between optimal control problem and viscosity solutions of Hamilton-Jacobi equations (see [7] for a comprehensive bibliography).

We recall that our goal is to directly discretize a particular Hamilton-Jacobi equation, the eikonal equation :

$$\|\nabla_x \tau(x)\|^2 = \frac{1}{c(x)^2} \tag{11}$$

where c denotes the speed of the medium and τ the travel time. In the hyperbolic equation terminology, rays are the characteristics of this equation. Classical solutions can generally be defined only in a neighborhood of the source. More precisely, up to the zone where rays cross. This is because the travel time becomes multi-valued when ray cross. It is always possible to define a single valued generalized solution called the viscosity solution. This solutions remains continuous but its gradient may be discontinuous. The locus of these singularities are the Hamilton-Jacobi counterparts of shocks for hyperbolic conservation laws. Stable upwind numerical finite difference schemes are known to converge to the viscosity solution. It is therefore the solution which can be computed using the Eikonal equation.

The following result (from [31]) is a by-product of theorems which can be found in [7] (see also [22]). We are interested in the viscosity solution of (9) for $x \in \Omega$, a fixed open domain. We supplement this equation with Dirichlet boundary conditions. We will split $\partial\Omega$ in two parts Γ, Γ_s ($\partial\Omega = \Gamma \cup \Gamma_s$) and we define the boundary conditions

$$\tau(x) = +\infty, \quad x \in \Gamma \tag{12}$$

$$\tau(x) = \phi(x), \quad x \in \Gamma_S \tag{13}$$

These conditions will be discussed at the end of the section.

Now τ the viscosity solution is the value function of the following exit-time optimal control problem, let y_x be the sate of the controlled dynamical system :

$$\begin{cases} \dfrac{dy_x}{dt} = -q(t), \ t \geq 0 \\ y_x(0) = x \end{cases} \tag{14}$$

where q the control can be taken in

$$A = \{q : R^+ \to R^{2,3} / \|q(t)\| \leq 1, \ t \geq 0\}.$$

The cost function is given by :

$$J(x,q) = \int_0^T \frac{1}{c(y_x(t))}\, dt + \phi(y_x(T)) \tag{15}$$

where T denotes the first exit time of Ω. i.e.

$$T = min\{t \geq 0 / \ y_x(t) \in \partial\Omega\}$$

and finally the viscosity solution of (9) (13) (12) is given by :

$$\tau(x) = \inf_{q \in \mathcal{A}} J(x, q). \tag{16}$$

Note that any smooth path $y_x(s)$ in Ω such that $y_x(0) = x$ and parameterized with its curvilinear abscissa s corresponds to an admissible control $q = dy_x/ds$. Conversely, given any admissible control $q(t)$ the constraint $\|q(t)\| \leq 1$ implies that a curvilinear "time" parameterization of the associated state (path) y_x gives an optimal cost (15). We have indeed :

$$\int_0^T \frac{1}{c(y_x(t))} \|q(t)\| dt + \phi(y_x(T)) \leq \int_0^T \frac{1}{c(y_x(t))} dt + \phi(y_x(T)). \tag{17}$$

So, after the change of variable for the curvilinear abscissa

$$s(t) = \int_0^t \|dy_x(u)\|,$$

we get $ds = \|dy_x/dt\| dt = \|q(t)\| dt$ and

$$\int_0^S \frac{1}{c(z_x(s))} ds + \phi(z_x(S)) \leq \int_0^T \frac{1}{c(y_x(t))} dt + \phi(y_x(T)) \tag{18}$$

where $z_x(s(t)) = y_x(t)$ and $S = s(T)$. This shows precisely that, for any control q the curvilinear "time" parameterization of the associated state (path) y_x is optimal (15).

The optimal control problem (16) can therefore be reformulated as the minimization of (15) (with t chosen to be the curvilinear abscissa) over all smooth path from x to the boundary $\partial\Omega$. More precisely we replace (16) with

$$\tau(x) = \inf_{y \in Y_x} G(y) \tag{19}$$

where

$$G(y) = \int_0^S \frac{1}{c(y(s))} ds + \phi(y(S)) \tag{20}$$

and

$$Y_x = \{y :]0, S] \to \Omega / y(0) = x \in \partial\Omega,\ y(S) \in \partial\Omega\} \tag{21}$$

For technical reasons, it will be more convenient to consider a backward parameterization $(y(s) = y(S - s))$. so that (21) becomes

$$Y_x = \{y : [0, S[\to \Omega / y(S) = x,\ y(0) \in \partial\Omega\} \tag{22}$$

and (20)

$$G(y) = \int_0^S \frac{1}{c(y(s))} ds + \phi(y(0)) \tag{23}$$

We now interpret in terms of rays the optimal paths of the above optimal control problem. We must keep in mind that the travel times along rays constitute the geometric solution. We therefore use the optimal control interpretation to identify the viscosity solution as different branches of the geometric solution.

1. We consider a bounded open domain Ω such that $x_0 \in \partial\Omega$. We set $\Gamma_S = \{x_0\}$ and $\Gamma = \partial\Omega \setminus \{x_0\}$. and take $\phi(x_0) = 0$ in (13), see figure (1). With this particular choice and in view of the cost function (20) any optimal path is constrained to start from point x_0. The optimal control is given by (19) (20) with

$$Y_x = \{y : [0, S[\rightarrow \Omega / y(S) = x,\ y(0) = x_0\} \tag{24}$$

   We now assume that there is a ray solution of (1), going from x_0 (the source point) to x, remaining strictly in Ω and realizing a minimum travel time with respect to all paths from x_0 to x remaining strictly in Ω. This ray is the path solution (exiting at x_0) of the optimal control problem and $\tau(x)$ is the minimum travel time from the source x_0 to x out of potential rays from x_0. Conversely any optimal path realizing a minimum for the cost function is a stationary point for the Fermat principle (4) (from x_0 to x). It is therefore a ray and the viscosity solution yields a travel time. Because of the boundedness of Ω the infimum may not be realized by a path. This would be the case for example if a minimizing sequence of path tends to some parts of the boundary $\partial\Omega$. There are, of course, no optimal path to be interpreted as a ray in this situation.

2. We now treat the case where Γ_S is not reduced to a point but is for instance a part of the boundary $\partial\Omega$. The optimal control is given by (19) (20) with

$$Y_x = \{y : [0, S[\rightarrow \Omega / y(S) = x,\ y(0) \in \Gamma_S\} \tag{25}$$

   The viscosity solution at x will then give the minimum travel time defined by (4) plus the initial value $\phi(x_0)$ (as in (15)) out of paths from x_0, a point of Γ_S, to x. If ϕ is defined as the trace on Γ_S of travel times specified by rays shot from a source point x_0 outside Ω, see figure (2). The optimal paths will be the continuations of the rays from the source points x_0 and entering Ω through Γ_S. One can actually check that the restriction of rays, which are global stationary point for the Fermat principle (from x_0 to x for example), to the domain Ω satisfy the transversality conditions ([19]) on Γ_S the initial surface and are therefore stationary of critical paths for (20). If we further assume the restricted rays are minima (as this will precisely be the case in section 3.2) then the viscosity solution gives the travel time specified by rays shot from the source.

Note that the result of this section holds with continuity hypothesis on ϕ. However, (as already mentioned) infinite exit cost problems as proposed here are studied as state constrained optimal control problems in [28] [32] (see also [7]). Even though the theoretical solution is discontinuous at such a boundary, numerical simulations and also theoretical results [2] show that, when taking sufficiently large ϕ as Dirichlet boundary condition, the

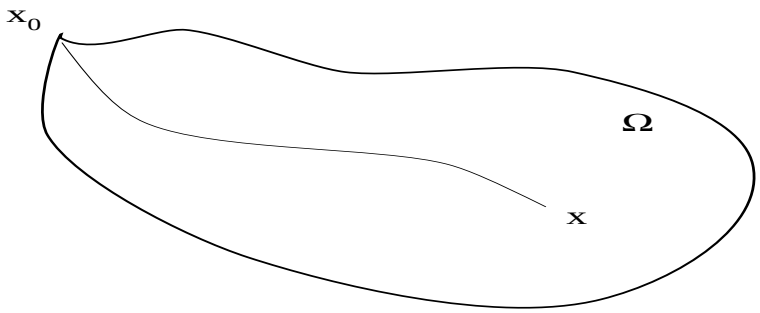

Figure 1: Travel time at point x given by the ray from x_0 (source) matches the viscosity solution in Ω with $\phi = +\infty$ on $\partial\Omega$ except at x_0 where $\phi = 0$ if this ray realize a minimum travel time out of all smooth path from x_0 to x in Ω.

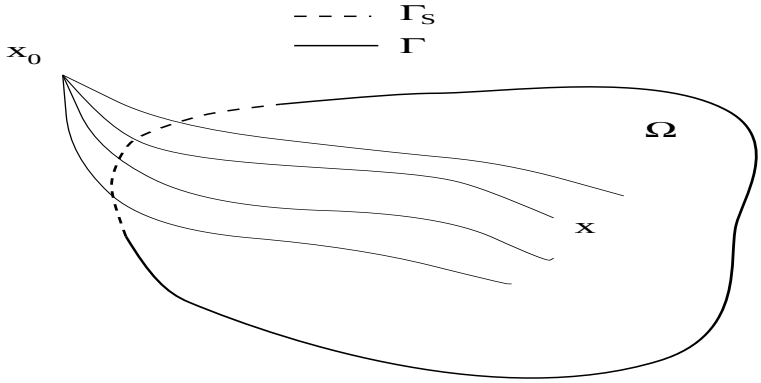

Figure 2: Travel time at point x given by the ray from x_0 (source) matches the viscosity solution in Ω with ϕ on Γ_S taken as the trace of travel times given by rays intersecting Γ_S and $\phi = +\infty$ on Γ if this ray realize a minimum travel time out of all smooth path from Γ_S to x in Ω with initial travel time specified by ϕ.

numerical solution converges towards the solution of the Dirichlet problem where ϕ would be given on all $\partial\Omega$ as the trace of τ defined by (16) in $\bar{\Omega}$. This quantity can be computed and we will use it in section 3.2.

2.3 BRT principle

BRT relies on the following remark illustrated in figure 3. One can see six rays and two (open) domains bounded respectively by (OAA')/(OBB') (plain lines) and (OBA)/(OB'A')

(dashed line). Two rays are crossing at point I giving two different travel times from point O. We assume that the two rays (thick lines) intersecting at I correspond to global minima for (4) with respect to paths restricted to lie in their respective domains and joining and I. In this situation the viscosity solutions, computed in each domain with boundary conditions as in section 2.2 2, will catch at point I two different waves (or branch) of the geometric solution of the eikonal equation.

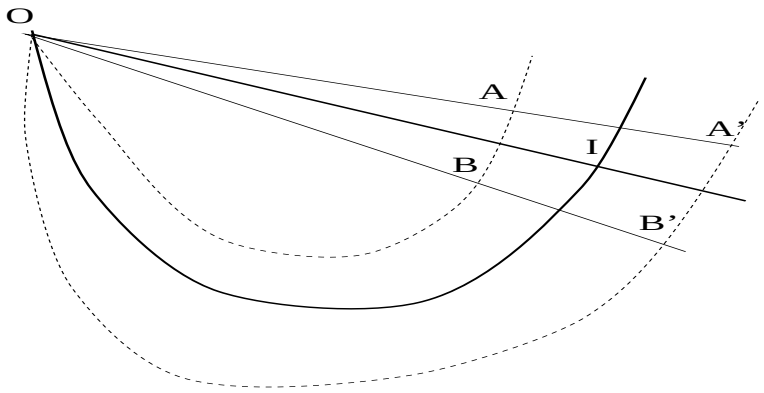

Figure 3: Two rays are crossing at I. One yield a first arrival time at the crossing I from the source O, the other a later arrival time. We assume the two rays are local minima for the minimum travel time problem (4). We assume that the two domains ((OAA')/(OBB') (plain lines) and (OBA)/(OB'A') (dashed line)) are such that each ray will be a global minimum its domain. The viscosity solutions in each domain will give the two different travel times at I.

2.4 A proposed algorithm

Based on the idea of section 2.3. The algorithm proposed in [9] consists in :

1. Tracing a given number of rays shot in regularly spaced initial directions.
2. Using a finite difference solver to compute the viscosity solution on a regular grid of the eikonal equation in restricted domains obtained by generating an envelope around two successively shot rays. We call these envelopes 'big rays'.
3. The travel time field is given by the superposition of all local travel time fields computed in the big rays. When big rays intersect (i.e. when rays are crossing), this process gives a multi-valued travel time field.

This procedure computes the multi-valued travel time at a given point if the ray tracing solution fulfill two conditions :

1. The rays crossing at that particular point have to be local minima for the Fermat principle. This mean in particular that their must be no conjugate point on the ray (see next section).

2. These rays, which are never actually traced, have to "live" in different big rays. This ensure that they will turn from local minima to global minima with respect to path constrained to lie in the considered domain. Hence the computed viscosity solution will yield the travel time associated with this particular ray.

2.5 Problems with BRT

We now consider a pathological case. In the presence of a caustic, the situation is different. A caustic is defined as the locus where the rays of the geometrical optics have an envelope (or a fold of the Lagrangian manifold in phase space ([18])). Caustic points are conjugate points, meaning that if a rays go through such a point (except for true focal points) it does not realize anymore a minimum travel time (4) from the source to points situated on the rays after the caustic. For points after the caustic one can always find a faster neighboring ray. This classical situation is represented in figure 4 where three rays hit a caustic (the thick line). We want to use two of them (plain lines) to build a big ray. We want to compute in particular the travel time associated with the ray (OC) (dashed line) after it has hit the caustic. We immediately see that the two conditions stated in section 2.4 are not satisfied. The region bounded by rays (OAIA') and (OBIB') is not connex and the ray (OC) is not strictly contained in this region. Even if we could construct a domain containing this ray it has a conjugate point (at the caustic) and therefore does not realize not a minimum, even though it is a stationary path for Fermat principle (4). Computing the viscosity solution of the eikonal equation in a region like (OIA'B'BAO) gives a wrong result in (IA'B'BI) as the upwind scheme takes the shortest "upwind" path along the boundary (OI) and there the infimum for the cost function (15) is not realized by a stationary path (ray).

This degenerate situation was part of the motivation for developing a corrected geometrical optic around caustics. We review rapidly this theory and use it to propose a corrected algorithm in the next section.

3 Geometrical theory of diffraction

3.1 Review of the theory

The geometrical theory of diffraction is an asymptotic approximation of the reduced wave equation which remains valid around caustics. More precisely it models correctly waves reflecting on the illuminated side of the caustics and also find an exponentially decreasing solution in the shadow region behind the caustic. We give here results which can be found (restricted to homogeneous media) in [23]. These results hold for smooth caustic and also smooth portions of cusp caustics. A more intuitive presentation of the theory is given in [21].

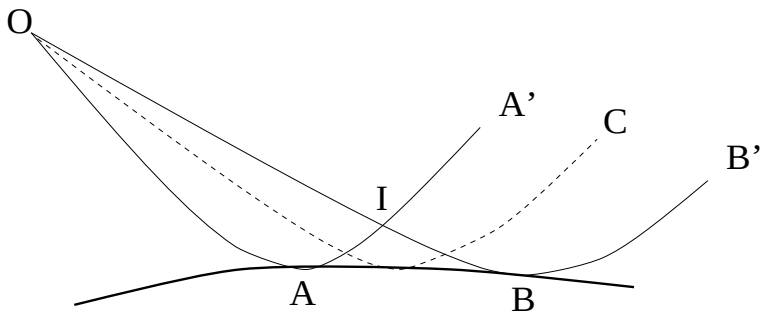

Figure 4: A caustic (thick line (AB)) and three rays reflected by the caustic. The problem is to define two local domains such that the viscosity solutions will yield the two different travel times in region (ABIA).

Using a different asymptotic solution of the wave equation (7), an approximated asymptotic representation of the solution on the illuminated side of the caustic (the side of point I on figure 4) is given by :

$$u(x) \sim \frac{\omega^{\frac{1}{6}}}{2\sqrt{\pi}} e^{-i\frac{\pi}{4}} (e^{i\omega\tau^+(x)} z^+(x) + e^{i\omega\tau^-(x)} z^-(x)) \tag{26}$$

There are two phases and two amplitudes in this expression. The $.^+$ quantities are associated to incoming wave and the $.^-$ quantities to the outgoing wave after it has touched the caustic. At point I on figure 4 for instance the travel time and amplitude associated to ray (OIB) is given by τ^+ and z^+, the travel time and amplitude associated to ray (OAI) is given by τ^- and z^-.

The travel times solve the same eikonal equations :

$$\|\nabla_x \tau^\pm(x)\|^2 = \frac{1}{c(x)^2}. \tag{27}$$

The amplitudes are given by (ρ is defined below) :

$$z^\pm(x) = \rho(x)^{-\frac{1}{4}} A^\pm(x)$$

where $A^\pm$ solve modified transport equations :

$$2\nabla_x \tau^\pm(x).\nabla_x A^\pm(x) + (\Delta\tau^\pm(x) \mp \frac{1}{2}\rho(x)^{-\frac{1}{2}}(\nabla_x \rho(x))^2) A^\pm(x) = 0 \tag{28}$$

The function ρ is taken strictly positive in the illuminated region and 0 on the caustic. It is given in terms of the phase functions $\tau^\pm$ and another variable θ by

$$\tau^\pm(x) = \theta \pm \frac{2}{3}\rho(x)^{\frac{3}{2}} \tag{29}$$

One sees that ρ depends on the difference between incoming and outgoing phase. We can eliminate θ and express ρ as a function of $\tau^{\pm}$. It is also important to notice that as ρ vanishes on the caustic we have there

$$\tau^{+}(x) = \tau^{-}(x). \tag{30}$$

All this is consistent with the fact that $\tau^{\pm}$ solve the classical eikonal equation and matches the travel time τ of classical geometrical optics respectively before and after rays hit the caustic. This is not true for the transport equations which incorporate an additional terms (compared to geometrical optics) such that amplitudes are well defined up to the caustic.

Note that a relation similar to (29) holds for the amplitudes :

$$A^{\pm}(x) = g_0(x) \pm \rho(x)^{\frac{1}{2}} g_1(x). \tag{31}$$

So that on the caustic we again have

$$A^{+}(x) = A^{-}(x). \tag{32}$$

This remark will prove useful in the perspective of computing amplitudes using BRT.

3.2 Unfolding the caustic

In section 2.4 we proposed an algorithm based on ray tracing. We want to correct it such that it can handle "degenerate" situations such as figure (4) (section 2.5).

To remedy to this situation, we first assume that we know the geometry of the caustic (segment going through A and B on figure (4)). We discuss in the next section how this information can be obtained.

We now remember that the caustic is the locus where the rays stop to realize local minima for the Fermat principle. It is therefore natural to cut the big ray using the caustic an restrain the computation of the viscosity solution in the domain (OAB). Then section 2.2. point 1 guarantees that the viscosity solution with the same boundary conditions matches travel time along the rays in this domain (in particular ray (OC)). We also notice that this travel time actually corresponds to τ^{-} of section 3. It is associated to incoming rays to the caustic.

We now use the trace of the travel-time on segment (AB) as a Dirichlet boundary condition (source) for a new resolution of the eikonal equation. We mean the travel time defined on (AB) by extending formula (19) to these points and not the infinite value of the Dirichlet boundary condition. This time we use the domain (AA'B'B) corresponding to outgoing rays from the caustic. The rays after the caustic are still stationary path for the new problem of minimal time from the caustic with fixed initial travel time on this surface. This is a direct consequence of the choice of the boundary condition as the trace of the travel time specified by the rays from the source which are themselves global stationary path (one can

actually verify the necessary transversality conditions [19]). The rays after the caustic are again minima for the Fermat principle because we passed the conjugate point (caustic) and we assume that we do not encounter a new one. In these conditions the viscosity solution matches travel times along these rays (and in particular for (CC'). It corresponds to τ^+ of section 3 (remember that $\tau^+ = \tau^-$ on the caustic).

What we implicitly did in these two separate computations is split the rays hitting the caustic, which globally corresponds only to stationary paths for the Fermat principle, in two parts. these two parts separately realize minima for the Fermat principle and therefore match the viscosity solution in their respective domain.

3.3 Reflection on boundaries

The same strategy can be in principle used to compute the wave reflected on boundaries. The boundaries are treated exactly as the caustic in the preceding section.

Figure 5 shows rays reflected by a boundary in an homogeneous medium. The thick lines represent the rays used to bound the domain where the viscosity solution is computed. Again two computations are performed. First in (OABO) with a point source condition at O and the infinite-exit-cost type boundary condition elsewhere. Then in (ABB'A'A) with the trace of the former computation as a source on (AB) and Soner boundary condition elsewhere.

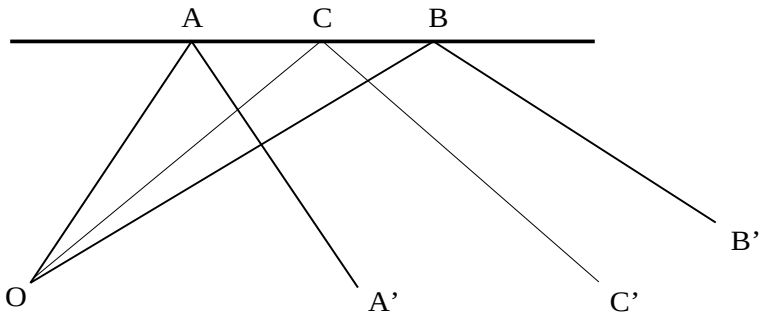

Figure 5: rays reflecting on a fixed boundary (thick line).

This method has of course a limited interest in the case of a single reflection in a homogeneous medium (the solution analytical is easily computed). This section however shows that the big ray tracing method can take into account, systematically and indiscriminately, multiple reflections on caustics and boundaries.

4 Description of the corrected BRT

4.1 Ray tracing

A ray tracing is first performed to get information on the structure of the geometric solution. This is usually done using a Runge Kutta algorithm on system (1) (2) for a fixed number of angle θ. We regularly sample the initial angular sector we are interested in.

4.2 computing the caustic

We want information on caustics in order to be able to split our computations at these points. Caustic points can be detected either using paraxial ray tracing or in principle by solving the transport equation.

Paraxial ray tracing ([14], [12]) is a method which estimate how linear perturbation $(\delta y(s), \delta p(s))$ in the initial condition propagate along a fixed ray $(y(s), p(s))$ solution of (1). It is extensively used for travel time interpolation between rays (see [15]).

Inserting $(y(s) + \delta y(s), p(s) + \delta p(s))$ in the same equations (1) we find that the perturbations (the paraxial quantities) satisfies in the first order approximation the differential equations :

$$\begin{cases} \dfrac{d\delta y}{ds} = \nabla_x \nabla_p H(y(s), p(s)).\delta y(s) + \nabla_p \nabla_p H(y(s), p(s)).\delta p(s) \\ \dfrac{d\delta p}{ds} = -\nabla_p \nabla_p H(y(s), p(s)).\delta y(s) - \nabla_p \nabla_x H(y(s), p(s)).\delta p(s) \end{cases} \tag{33}$$

where H is given by (5).

In the case of a 2-D point source problem 1 2 the rays depends both on the "time" parameterization and the angle θ of the initial condition. The determinant of the Jacobian matrix

$$\frac{\partial y(s,\theta)}{\partial(s,\theta)}$$

gives a measure of the deformation of a infinitesimal tube $\delta\theta_0(s) \times \delta s_0(s)$ along the ray.

The amplitude $A_0(s)$ transported along the ray is weighted by the geometrical spreading

$$J(s) = \frac{1}{c(y(s))} |det(\frac{\partial y(s,\theta)}{\partial(s,\theta)}|. \tag{34}$$

It is given by

$$A_0(s) = A_0(0)\sqrt{\frac{J(0)}{J(s)}}. \tag{35}$$

when J vanishes the amplitudes blows up (the ray tube collapse), the rays hits a caustic. The computation of J is performed using paraxial ray tracing (33). It simply suffices to identify

δy with respectively $\frac{\partial y}{\partial s}$ and $\frac{\partial y}{\partial \theta}$ and use the correct initial conditions. In the case of an isotropic point source (2) $\frac{\partial y}{\partial s}$ is given by solving (33) with initial conditions $\delta y(0) = (cos(\theta), sin(\theta))$ $\delta p(0) = (0,0)$ and $\frac{\partial y}{\partial \theta}$ is given by the same equation with initial conditions $\delta y(0) = (0,0)$ $\delta p(0) = (-sin(\theta), cos(\theta))$.

The geometry of caustics can be obtained that by shooting a sufficient number of rays and their paraxial quantities. This may seem prohibitive as we precisely want to avoid ray tracing. We note however that caustics are envelope of rays and therefore rays will have a tendency to concentrate there so that even a small number of rays will catch their geometry. If not the caustic is touched by few tangent rays so that multiple travel time only occur close to it. We will ignore these under sampled caustics assuming in this work that one of this ray is a good approximation of the geometry of the caustic and of the travel times of the different rays in the vicinity of the caustic. This mean that the earliest single valued travel time computed by standard BRT (without considering the caustic) will be accurate enough. A rigorous approach of this problem would certainly depend on the interpretation of Ludwig/Keller ansatz for cusp caustics [23] in terms of multi valued travel times and is discussed in section 4.3 point 4.

It should also be mentioned that even using a large number of ray, the recovery of the geometric solution on a regular grid using interpolation procedures is non trivial. The problem with ray tracing is not its cost but its inability to systematically compute the multi valued travel time field on a regular grid.

An other option would be to solve the transport equation (10) and detect where the amplitude blows up. In this case however and like for the eikonal equation we need to define a domain and boundary condition. Special care should be taken in the case of multiple successive caustics as it is not possible to solve (10) beyond caustics. We discuss these points in section 5.1.

4.3 Creating the big rays

We now assume that we are given a number of rays and the geometry of the different caustics. The caustic points computed by paraxial ray tracing are interpolated on the finite difference grid for the Eikonal equation as well as two successively shot rays. These points will constitute the discrete boundaries of our big rays. Under-sampled caustics represented only by sparse points are ignored.

We further suppose that the caustic history of each ray is known. The BRT algorithm now consists in selecting two successively shot rays.

1. If these two rays have not touched any caustic, they necessarily do not cross and we define the big rays as the envelope of these two rays. This envelope potentially contains all rays with initial direction comprised between the two considered rays. If

multi-valuedness occurs inside this big ray then only the first arrival time is computed. We say that we miss small scale multi-valuedness.

2. When the two rays touch a smooth part of the same caustic. We use the procedure described in section 3.2. We first solve in the region bounded by the incoming rays at the caustic and the segment of caustic itself and use the trace of travel time on this segment as a source and the remaining part of the two rays to iterate the process of big ray tracing. The remaining part of the rays can indeed again encounter one of the three present situations.

3. One of the ray touches a caustic and not the other.the two rays The building rays do not cross and we ignore the caustic. The computed travel time will give first arrival in the envelope. It will in particular compute rays "crawling" under the caustic. We can miss travel times associated to some parts of the direct rays (before they hit the caustic) and reflected rays (after).

4. The two rays touch smooth parts of the same caustic separated by a singularity (cusp). In the current implemented version of our algorithm this situation is not taken into account. In the numerical simulation (section 6) presented we are indeed in the situation of cusp caustic. But only one smooth part of the caustic is identified because very few rays touch the other part. We chose to ignore this part of the caustic (section 4.2) and forget about the multiple travel times.

   The following remarks however gives indication on what should be done to take this situation into account in our algorithm :

   The rays cross before both of they have touched the caustic. Four computations should be done in that case. they are depicted in figure 6. First before the cusp in the single travel time zone bounded by rays (a). We keep the trace of travel time on the caustic. Then in each zone bounded by one ray and the caustic with source term on the smooth part of the caustic crossed by the rays and Soner BC on the remaining part of the caustic. Finally in the multi valued zone bounded by the caustic and the rays with only a source point at the singularity.

   The rays cross before both of them graze the caustic. Four computations should be done in that case. they are depicted in figure 6. First before the cusp in the single travel time zone bounded by rays and the cusp. We keep the trace of travel time on the caustic. Then, after the caustic in each zone bounded by one ray and the caustic with source term on the smooth part of the caustic crossed by the rays and Soner BC on the remaining part of the caustic (separated by the caustic singularity). This step compute traveltimes associated to rays which have first crossed one part of the caustic until they graze the other part of the caustic. Then you again keep the trace of traveltime on the caustic given by this new computations and Finally in the zone

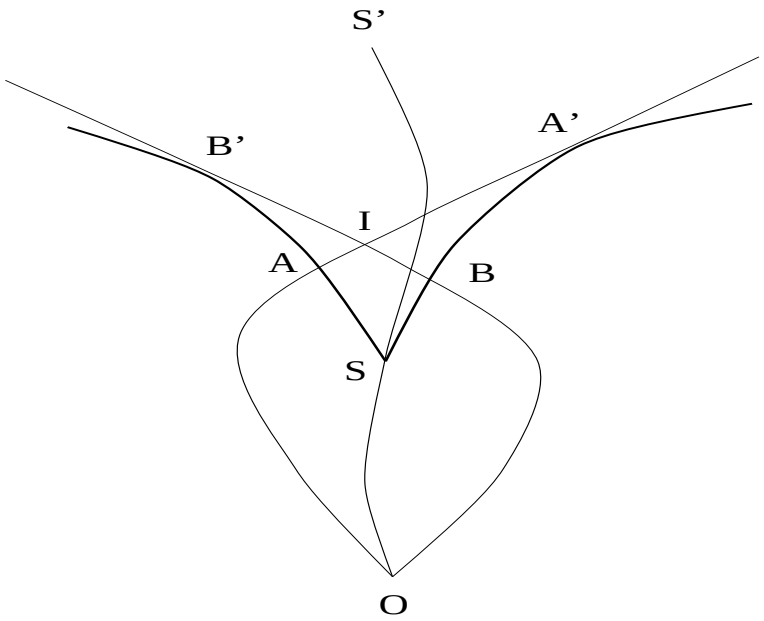

Figure 6: Rays (OAA') and ray (OBB') cross before they touch the caustic (thick line). There are also rays (0SS') going through the singularity of the caustic S. These rays cross at S with the same travel time. In this case S is also the starting point of the gradient singularity of the global viscosity solution. We first solve in (OASBO) (before the caustics) with source point at O and keep the trace of travel time for further computations. Then we solve in (SB'BS) with source specified on (SB) (S excluded) by the previous step and likewise on (SA'AS) with source on (SA). Finally we must solve after the caustic with dirichlet source on the caustic given by the trace of the last computation.

bounded by the caustic (after the caustic) you use this trace a new Dirichlet boundary condition and you find the later arrival of the triplication.

In this section we defined an automatic procedure to compute multi valued travel times. The goal is to compute the geometric solution on a regular grid using few solve of the eikonal equation. The idea is therefore to use the smallest possible number of big rays without loosing information on multi-valuedness. We present a numerical test in section 6 to prove the tractability of our approach.

4.4 An upwind scheme for the eikonal equation

We present here for the sake of completeness a numerical scheme for the eikonal equation which can be found in ([31]).

The derivation of the scheme is based on the remark that the viscosity solution τ of (9) satisfy :

$$\|\nabla_x \tau(x)\|^2 = \frac{1}{c(x)^2} \Leftrightarrow \sup_{\|q\|\leq 1} \{\nabla_x \tau(x).q - \frac{1}{c(x)}\} = 0, \ \forall x \in \Omega. \tag{36}$$

τ is given on $\partial\Omega$ by Dirichlet boundary conditions ((13) and (12) for example).

A regular grid discretization of the domain Ω is introduced and note $(x_i, y_j) = (i\Delta x, j\Delta y)$ the points of this grid. τ_{ij} will be the value of the discrete approximation of τ at (x_i, y_j). We also define the following index sets‘:

$$Q = \{(i,j) \in N^2 / (x_i, y_j) \in \Omega\}$$

the restriction of the grid to the domain Ω and

$$\partial Q = \{(i,j) \in N^2 / \partial\Omega \cap](i-1)\Delta x, (i+1)\Delta x[\times](j-1)\Delta y, (j+1)\Delta y[\neq \emptyset\}$$

a discrete approximation of the boundary $\partial\Omega$.

A first order finite difference approximation is made in (36) :

$$\sup_{\|q\|\leq 1} \{\frac{\tau(x - \Delta t q) - \tau(x)}{-\Delta t} - \frac{1}{c(x)}\} = 0 \tag{37}$$

The equation will be written at $x = (x_i, y_j)$ with $\Delta t = \frac{\Delta x \Delta y}{\sqrt{\Delta x^2 + \Delta y^2}}$. A convex linear approximation is made for $\tau(x - \Delta t q)$. More precisely if

$$(x - \Delta t q) \in](i)\Delta x, (i+1)\Delta x[\times](j)\Delta y, (j+1)\Delta y[$$

for example we will use the approximation

$$\tau(x - \Delta t q) = \alpha\, \tau_{ij} + \beta\, \tau_{i+1j} + \gamma\, \tau_{ij+1}$$

where a, b, c are such that

$$\begin{cases} x - \Delta t q = \alpha\,(x_i, y_j) + \beta\,(x_{i+1}, y_j) + \gamma\,(x_{i+1}, y_{j+1})) \\ \alpha + \beta + \gamma = 1 \end{cases}$$

using these expression in (37) we can obtain an analytical expression for the supremum in term of a discrete Hamiltonian :

$$g_{ij}(a,b,c,d) = \sqrt{max(a^+, b^-)^2 + max(c^+, d^-)^2} - \frac{1}{c(x_i, y_j)} \tag{38}$$

where $a^+ = max(0, a)$ and $b^- = max(0, -b)$. This numerical Hamiltonian picks up the upwind discretization of the gradient of travel time. By upwind we mean the direction of the characteristic (ray) giving the earliest travel time. This choice prevents spurious

oscillations along shocks (zones where rays cross with same travel time and discontinuous gradient).

Then a numerical discrete approximation of τ satisfies

$$\begin{cases} \tau_{ij} = \phi(x_i, y_j),\ \forall (i,j) \in \partial Q \\ g_{ij}(D_x^- \tau_{ij}, D_x^+ \tau_{ij}, D_y^- \tau_{ij}, D_y^+ \tau_{ij}),\ \forall (i,j) \in Q \end{cases} \tag{39}$$

with

$$\begin{cases} D_x^- \tau_{ij} = \frac{\tau_{ij} - \tau_{i-1\,j}}{\Delta x} \\ D_x^+ \tau_{ij} = \frac{\tau_{i+1\,j} - \tau_{ij}}{\Delta x} \\ D_y^- \tau_{ij} = \frac{\tau_{ij} - \tau_{ij-1}}{\Delta y} \\ D_y^+ \tau_{ij} = \frac{\tau_{ij+1} - \tau_{ij}}{\Delta y} \end{cases} \tag{40}$$

The convergence of this discrete solution toward the continuous viscosity solution as the mesh size goes to zero is proved in [31]. The theoretical accuracy is proportional to $\sqrt{\Delta t}$ but in practice one observes a first order accuracy.

Let G be the operator defined on the space of all $\Theta = (\tau_{ij}^0)_{(i,j)\in Q \cup \partial Q}$:

$$G(\Theta)_{ij} = g_{ij}(D_x^- \tau_{ij}, D_x^+ \tau_{ij}, D_y^- \tau_{ij}, D_y^+ \tau_{ij})$$

The problem is now find the discrete field Θ satisfying $G(\Theta) = 0$ and the boundary condition $\tau_{ij} = \phi(x_i, y_j),\ \forall (i,j) \in \partial Q$. We use a relaxation algorithm proposed in [26] and described in [31]. It simply consist in:

1. Step $n = 0$: choose $\Theta^0 = (\tau_{ij}^0)_{(i,j)\in Q\cup\partial Q}$ such that $\tau_{ij}^0 = \phi(x_i, y_j)$ for all $(i,j) \in \partial Q$ and $G(\Theta^0) \leq 0$.
2. Step $n+1$: for all $(i,j) \in Q$, set $\tau_{ij}^{n+1} = sup\{u\ s.t.\ G(V) = 0\ where\ V_{ij} = u\ and\ V_{kl} = \tau_{kl}^n\ for\ (kl) \neq (ij)\}$

The particular form of G enable to compute analytically the solution of the relaxed equation (step $n+1$). Again the convergence of this algorithm is proved in [31]. It was found to be much faster than more classical algorithms looking for stationary or fixed point solution of a "time" dependent equation. In practice we observed a convergence proportional the largest size of the grid.

Other upwind schemes for Hamilton Jacobi equations can be found in [24] [27]. A Hamilton Jacobi solver on unstructured meshes is proposed in [1] [2]. It has been combined with BRT in [3].

5 Further considerations

5.1 Solving the transport equation

We give here ideas related to the numerical resolution of the transport equations (10) (28). If we note $A = log(A_0)$ or $A = log(A^{\pm})$ (the amplitude can undergo large variations) both

equations can be rewritten

$$\nabla_x \tau(x).\nabla_x A(x) = K(x) \tag{41}$$

Where

$$K(x) = -\frac{1}{2}\Delta\tau(x)$$

for (10) and

$$\begin{cases} \tau(x) = \tau^{\pm}(x) \\ K(x) = \Delta\tau^{\pm}(x) \mp \frac{1}{2}\rho(x)^{-\frac{1}{2}}(\nabla_x \rho(x))^2 \\ \rho(x) = \frac{1}{8}(3\tau^{+}(x) - 3\tau^{-}(x))^{\frac{3}{2}} \end{cases}$$

for (28)

The main idea for solving the transport equation is to chose an upwind discretization of the gradient of the amplitude. This choice prevents spurious oscillations and is natural as the characteristics (rays) precisely transports the amplitude (by upwind we mean here the upwind direction of travel time). There are no need for boundary conditions except for the source terms (like for the Eikonal equation). With the notation of section 4.4. An upwind discretization of (41) (in the same spirit as in [31]) could be written as

$$\{(D_x^- \tau_{ij})^+ D_x^- A_{ij} + (D_x^+ \tau_{ij})^- D_x^- A_{ij}\} + \{(D_y^- \tau_{ij})^+ D_y^- A_{ij} + (D_y^+ \tau_{ij})^- D_y^- A_{ij}\} + = K_{ij} \tag{42}$$

Then I suppose one could use a relaxation scheme as in section 4.4. and look at the convergence.

In (42) K_{ij} is a discrete approximation of K. The problem of the approximation of this term is discussed in [13] [30]. The authors recommend the use of higher order scheme (preferably third order) for the travel time as K involves second derivatives of the travel time. Higher (ENO) schemes for Hamilton-Jacobi equation can be found in [24] [27]. They rely on a higher order approximation for the fluxes $(D_x^- \tau_{ij}, D_x^+ \tau_{ij}, D_y^+ \tau_{ij}, D_y^- \tau_{ij})$.

5.2 A proposal for Dynamic BRT

As mentioned in section 4.2. One can also imagine to use the transport equation (41) to locate caustics. This procedure could be included in an algorithm we call Dynamic BRT. It relies on the idea that travel time computations, amplitudes computations and determination of caustics can be performed dynamically in the BRT algorithm.

The upwind scheme for the eikonal equation actually computes travel time along the rays. Amplitude given by the transport equation of geometrical optics (10) can be computed at the same time as it needs the upwind direction of travel time. In case 1 of section 4.3 this procedure will give a single valued travel time and the correct amplitude (there are no caustics).

When the big ray touches a caustic (case 2 section 4.3), the solution of (10) will blow up along the caustic. We should therefore be able to stop the computation along these points and we obtain τ^- (see section 3). We can then proceed in the remaining part of the big rays as proposed in section 3.2. We then obtain τ^+. We now have the necessary quantities to correct the amplitudes as proposed by the geometrical theory of diffraction. We can solve (28) in each part of the big ray using the trace of the amplitude on the caustic for the second part of the big ray (remember that $A^+ = A^-$ there).

Case 3 (section 4.3) ignores the caustics so we should stick to classical geometrical optics and admit we make an error there. Case 4 should be treated by analogy with case 2.

5.3 Remarks on 3-D extension

All the material presented in this paper obviously concerns 2-D computations. Ray tracing and numerical schemes for the Eikonal and transport equation in 3-D is not a problem. The main difficulty will be the big ray construction. First because rays remain paths and we need surfaces to bound the domain. second because caustics will probably be more difficult to locate. It should be noted however that because we use outgoing (Soner or infinite exit cost) boundary conditions the geometry of the big ray need not be very accurate. The only requirement is that it is a "reasonable" envelope of the rays corresponding to the travel time we want to compute. The determination of caustic will probably be easier using the procedure described in section 5.2.

Finally, let us mention the algorithm (in 3-D) developed in [10] where the set of initial take-off angle for the rays (ray domain) is automatically partitioned in zones associated to rays with the same "history". This notion is close to the idea of big ray developed here.

6 Numerical Results

- Figure (7): A stratified (vertically) velocity medium (c) starting at 1 and jumping smoothly at 3.
- Figure (8): 50 rays shot in this medium. There is a low density zones and a triplication zones bounded by a cusp caustic. The triplication is formed by the direct rays, the rays reflected on the caustic and rays crawling under the caustic (missing here) and filling the low density zone before going back to the bottom. A much finer ray tracing would be needed to fill up that zone.
- Figure (9): Contour line of travel time (every $0.02s$.) of the associated viscosity solution in all the domain. The shock can be observed precisely where the crawling rays will meet the direct ray with same travel time. This computation indicate the first arrival fronts. Note that the shock only touches the caustic at its singular point.

- Figure (10): Caustic points computed by paraxial ray tracing and interpolated on a regular 100×100 grid. We will ignore the under sampled part of the caustic.
- Figure (11): A first solution of the Eikonal equation in a domain bounded by the first ray to touch the caustic (the smooth part of the caustic we keep for our computation). Source point at $(0, 0)$, infinite Dirichlet B.C. elsewhere. These are contour line of travel time (every $0.02s$.).
- Figure (12): Two computations. Left : the viscosity solution in the domain bounded by the same ray until it touches the caustic. Source point at $(0, 0)$, infinite Dirichlet B.C. elsewhere. Right : the viscosity solution in the domain bounded by the remaining part of the ray and the caustic. Source specified on the caustic by the travel time of the former computation on the caustic, infinite Dirichlet B.C. elsewhere. These are contour line of travel time (every $0.02s$.).
- Figure (13): All the travel times together.
- Figure (14): Travel time traces on an horizontal line (at 0.2), the vertical axis is the time of arrival. Left computed using 500 rays. Right the trace of our viscosity solutions. We observe the direct first arrival, the reflected arrival and in between the arrival associated to crawling rays. The ray tracing solution miss these travel times (low density zone).
- Figure (15): Comparison between the two preceding computations. Note the inaccuracy of the viscosity solution at the left end of the latest arrival. Remember we ignored the under sampled part of the caustic so that we are missing rays in this area.

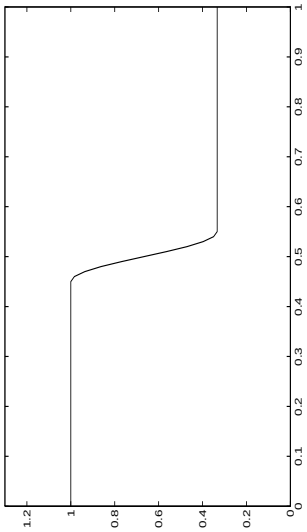

Figure 7:

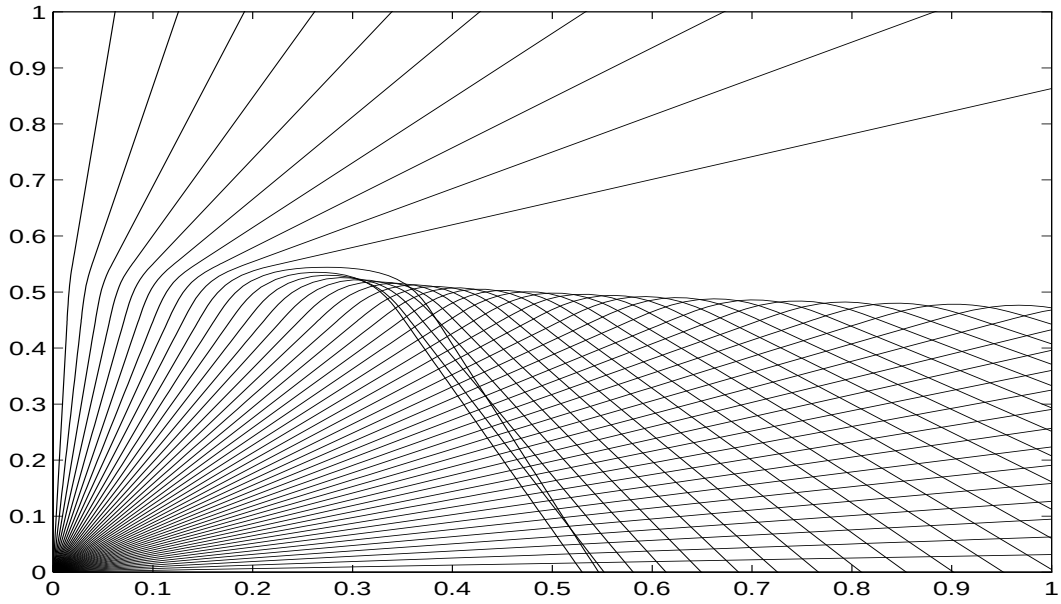

Figure 8:

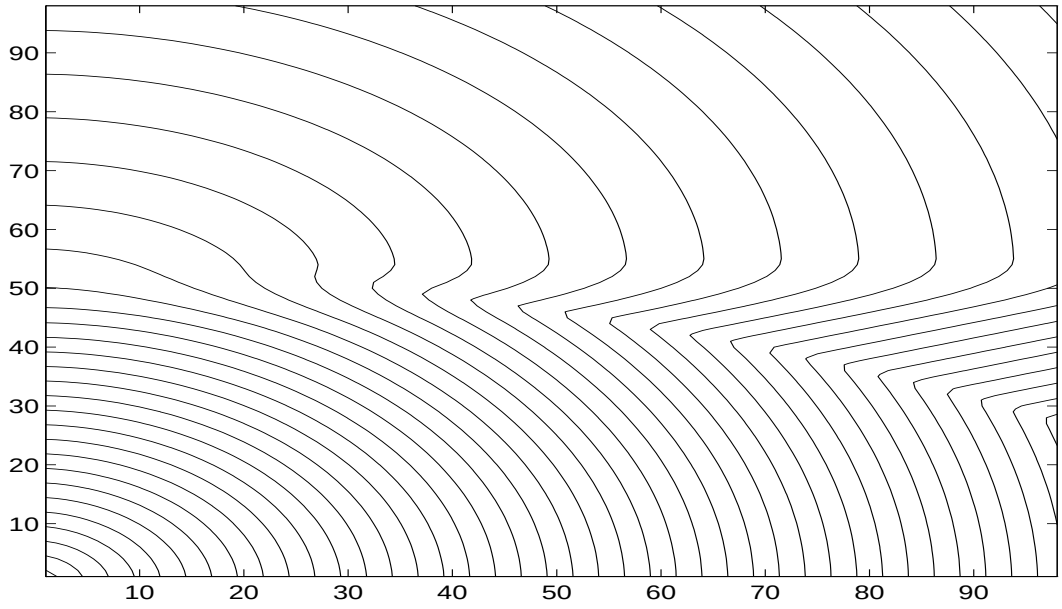

Figure 9:

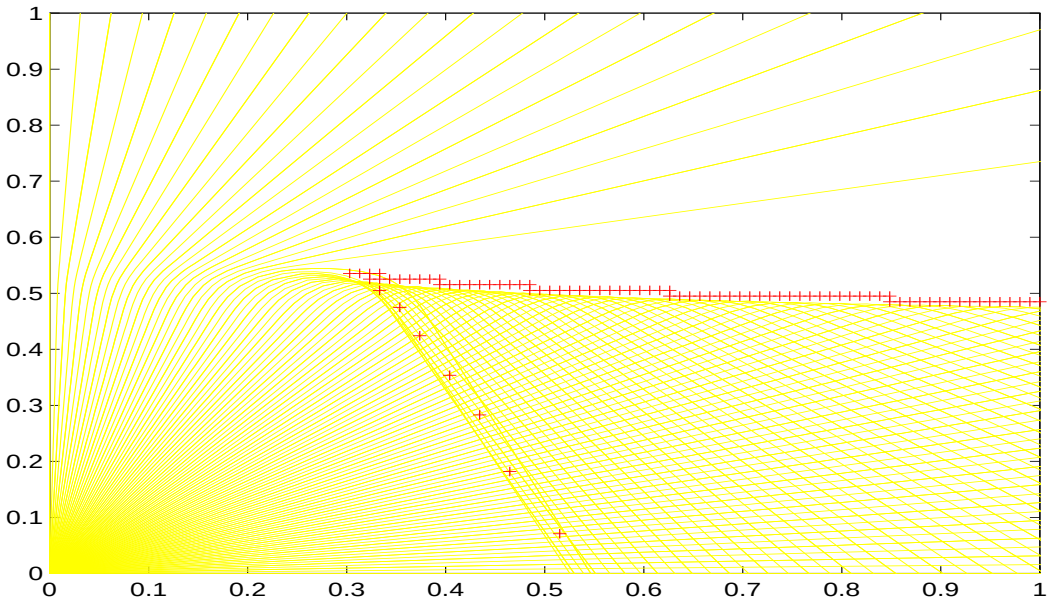

Figure 10:

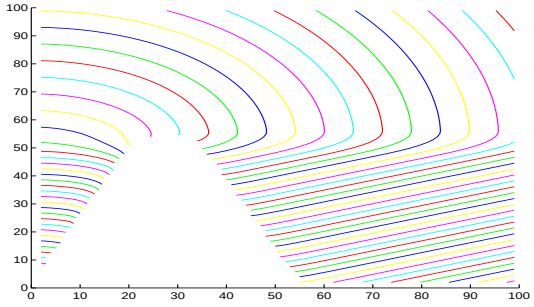

Figure 11:

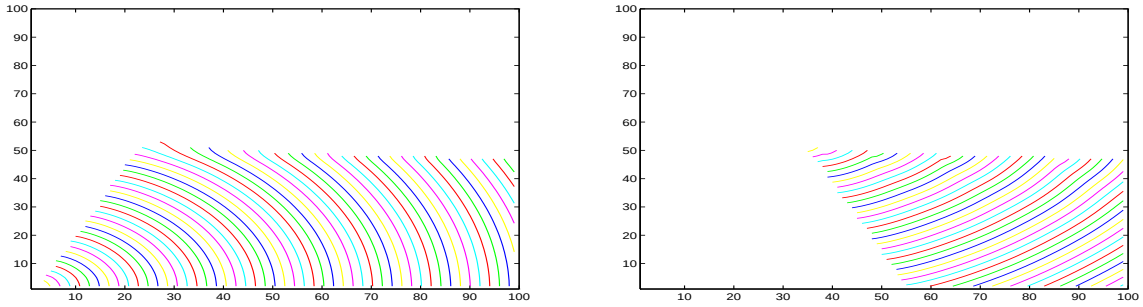

Figure 12:

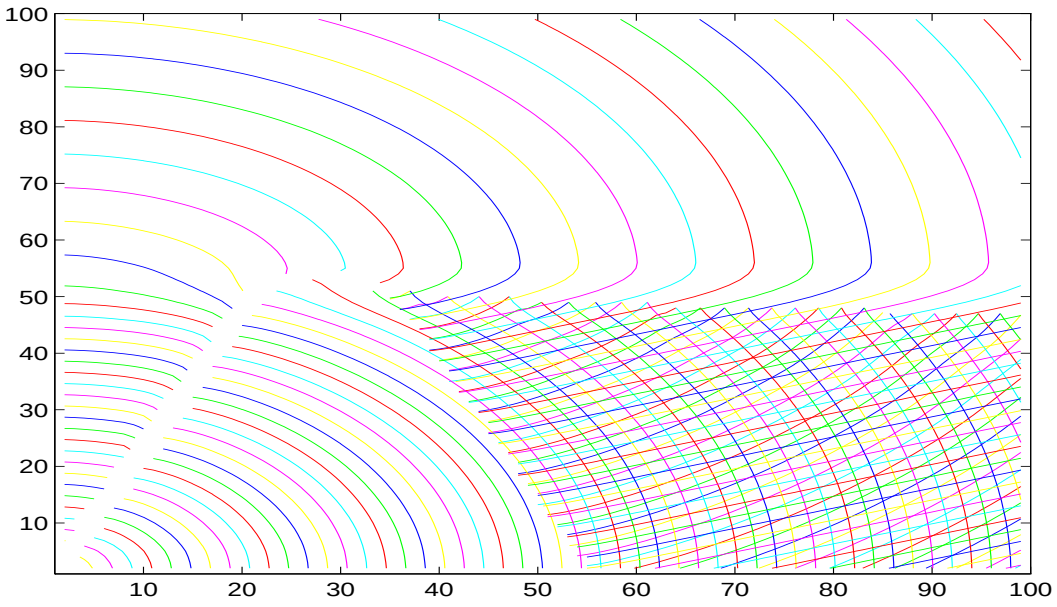

Figure 13:

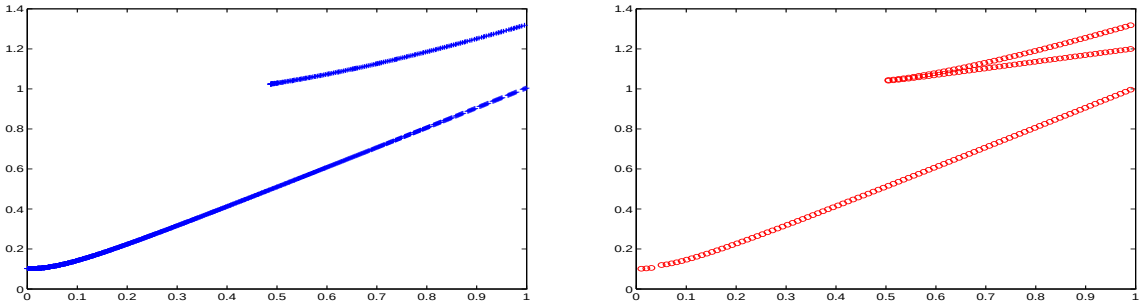

Figure 14:

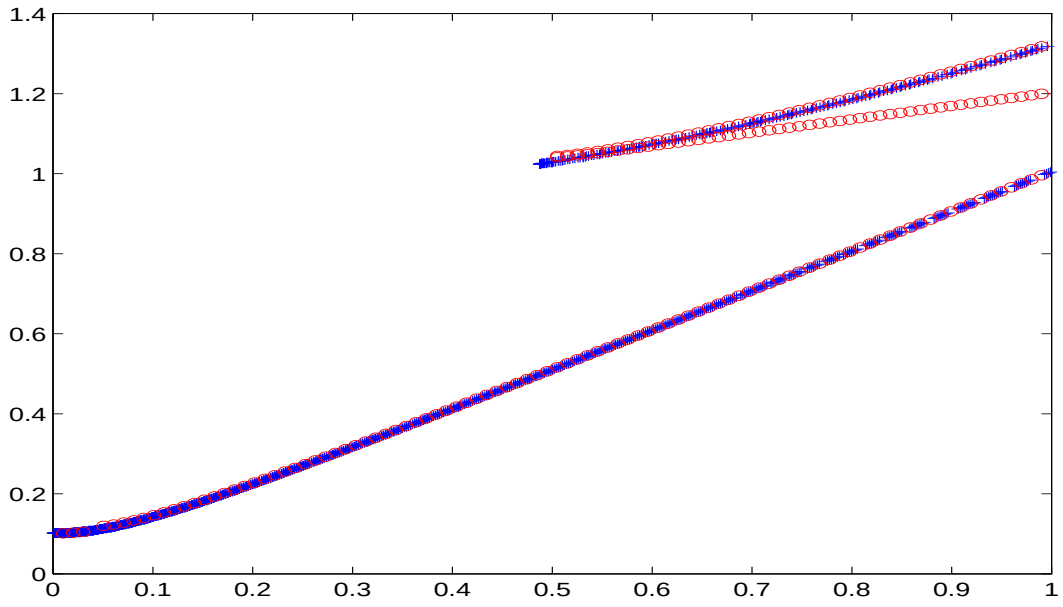

Figure 15:

7 Conclusion

The key idea of this report can simply expressed by the following concluding remark :

The geometric solution, that is the multi valued solution obtained by ray tracing is associated to stationary (or critical) paths (precisely the rays) for the Fermat principle. The Fermat principle is indeed an optimal control problem with a cost function depending on path and giving the travel time. On the other hand the viscosity solution of the Eikonal equation (computed by upwind numerical schemes) can be expressed using the same optimal control problem. The main difference being that the solution is associated to paths minimizing the cost function (that is the travel time) under source and state (domain) constraints. The situation is not desperate as rays can also be (sometimes local) minima or made of portions of minima separated by caustic points.

The proposed solution is first to use a coarse ray tracing to define local zones (BRT). This step aims at converting rays which are local minima into global minima under the constraint that path have to remain locally around that particular ray. The second step is to split the computations at caustics to ensure that the different part of the rays will match minimum path before and after the caustic in two different zones. The numerical simulation confirms that everything works fine for smooth parts of caustics. Special care should be taken near the singularity of cusp caustics (section 4.3).

Adding the computation of amplitudes should improve the procedure to locate caustics and also enables to correct amplitudes near caustics according to the geometrical theory of diffraction.

Acknowledgments

The author is grateful to G. Kossioris and G. Makrakis for fruitful discussions.

8 Review of different methods

This section is independent from the remaining part of the report. Some of its material have already been exposed in the first part.

We first discuss the relation between viscosity solutions of the eikonal equation and standard ray tracing. Viscosity solution is the correct notion of solution computed by stable upwind numerical solvers (details and references on numerical solvers for Hamilton-Jacobi equations can be found in [31] [24] [27] [1] [2]) . This relation is then used to present the ideas underlying three different methods proposed to compute multi-valued travel time fields using viscosity solutions. All these methods are hybrid in the sense they rely on some other "mechanism" to compute the geometric solution. This hybridization offers a potential for parallelization.

8.1 Viscosity solutions of the eikonal equation

A voluminous literature is available on the relations between optimal control problem and viscosity solutions of Hamilton-Jacobi equations (see [7] for a comprehensive bibliography).

We recall that the pursued objective is to directly discretize the eikonal equation

$$\|\nabla_x \tau(x)\|^2 = \frac{1}{c(x)^2} \tag{43}$$

where c denotes the speed of the medium and τ the travel time. In the hyperbolic equation terminology, rays are the characteristics of this equation. Classical solutions can generally be defined only in a neighborhood of the source. More precisely, up to the zones where rays cross. This is because the travel time becomes multi-valued when ray cross. It is possible to define a single valued generalized solution called the viscosity solution [22]. These solutions remains continuous but its gradient may be discontinuous. The locus of these singularities are the Hamilton-Jacobi counterparts of shocks for hyperbolic conservation laws. Stable upwind numerical finite difference schemes are known to converge to the viscosity solution.

The following result (from [31]) is a by-product of theorems which can be found in [7] (see also [22]). We are interested in the viscosity solution of (43) for $x \in \Omega$, a fixed domain. We supplement this equation with a Dirichlet boundary condition

$$\tau(x) = \phi(x), \quad x \in \partial\Omega. \tag{44}$$

Then τ (the viscosity solution) is the value function of the following exit-time optimal control problem : let y_x be the sate of the controlled dynamical system :

$$\begin{cases} \dfrac{dy_x}{dt} = -q(t), \ t \geq 0 \\ y_x(0) = x \end{cases} \tag{45}$$

where q the control can be taken in

$$A = \{q : R^+ \to R^{2,3} / \|q(t)\| \leq 1, \ t \geq 0\}.$$

The cost function is given by :

$$J(x,q) = \int_0^T \frac{1}{c(y_x(t))}\,dt + \phi(y_x(T)) \tag{46}$$

where T denotes the first exit time of Ω. i.e.

$$T = min\{t \geq 0/\ y_x(t) \in \partial\Omega\}$$

and finally the viscosity solution of (43) (44) is given by :

$$\tau(x) = \inf_{q \in \mathcal{A}} J(x,q). \tag{47}$$

Note that any C^1 path $y_x(s)$ in Ω such that $y_x(0) = x$ and parameterized with its curvilinear abscissa s corresponds to an admissible control $q = dy_x/ds$. Conversely, given any admissible control $q(t)$ the constraint $\|q(t)\| \leq 1$ implies that a curvilinear "time" parameterization of the associated state (path) y_x gives a lower cost (46). The optimal control problem (47) can therefore be formulated as the minimization of (46) (with t chosen to be the curvilinear abscissa) over all path from x to the boundary $\partial\Omega$.

We now distinguish three cases :

1. This results holds when $\Omega = R^{2,3} \setminus \{x_0\}$ is unbounded. In this case x_0 is a source point, (44) reduces to
$$\tau(x_0) = 0 \tag{48}$$
and every optimal path from x necessarily "exit" at x_0. The cost function (46) is given by
$$J(x,q) = \int_0^T \frac{1}{c(y_x(t))}\,dt \tag{49}$$
and the optimal control problem is nothing but the Fermat (minimum travel time) principle. It can be shown (rigorously) that the optimal path y_x with a suitable backward time parameterization s (here exactly the travel time) satisfy the ray (Euler) equations :
$$\begin{cases} \dfrac{dy}{ds} = pc(y)^2 \\ \dfrac{dp}{ds} = p^2 c(y) \nabla_x c(y) \end{cases} \tag{50}$$
supplemented by a two point initial and final conditions. In this case (47) indicates that the viscosity solution will pick up at one point the earliest travel time out of potential rays (characteristics) crossing there. The solution will remain continuous will possible discontinuities in the gradient where rays cross with matching travel times.

2. We now consider a bounded Ω and take $\phi(x_0) = 0$ for $x_0 \in \partial\Omega$ and $\phi = +\infty$ elsewhere $\partial\Omega$ (this choice actually corresponds to a state constrained optimal control problem [28] [32]). We assume that there is a ray solution of (50), going from x_0 to x, remaining strictly in Ω and realizing a minimum travel time in the sense of (49). With our boundary condition and in view of the cost function (46) any optimal path is constrained to exit the domain at x_0. Parameterized with its curvilinear abscissa, this ray is the path solution of the above optimal control problem (47) and $\tau(x)$ is the minimum travel time from the source x_0 to x out of every potential path from x to $\partial\Omega$.

3. Finally, it is possible to give a prescribed finite value to the boundary condition ϕ on a fixed part S of the boundary $\partial\Omega$ and $+\infty$ elsewhere. In an unbounded domain (case 1) the source can also be specified on an hyper-surface S. The viscosity solution at x will then give the minimum travel time out of paths from x to x_0 on S. The optimal paths will be rays from source points x_0 on S with initial travel-time given by $\phi(x_0)$.

We summarize this section by the following principle : "The travel time specified by a ray at a point will match the viscosity solution if the ray between the source and the considered point realize the minimum travel time out of all paths starting at that point and exiting the domain at a source point ."

8.2 hybrid methods

We now consider the simple situation (figure 16) where two rays (R1 and R2) are crossing at point I giving two different travel times $t1$ and $t2$. We further assume that $t2 < t1$. We present ideas underlying three different ways of computing these two travel times without tracing rays (R1, R2) and using viscosity solution of the eikonal equation (computed by a suitable discretization of (43)). More on these methods can be found in in [6] [5] for section 3.1, [29] for section 3.2 and [9] [8] for section 3.3. The computation of the multi-valued travel time field in a realistic seismic model using this last method can also be found in [3].

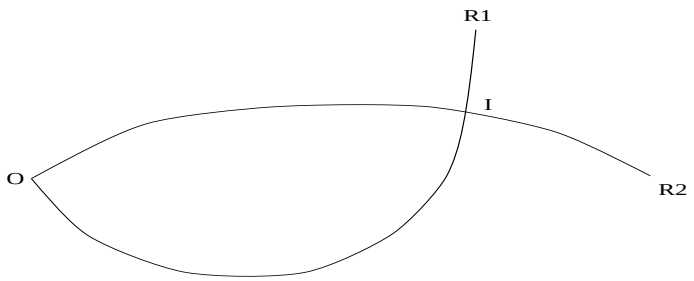

Figure 16:

8.3 A gradient singularity-capturing based algorithm

The hyperbolic conservation law community has a long experience of shock capturing. That is finding precisely where the viscosity solution is discontinuous without tracing the characteristics. In the case of Hamilton Jacobi equations we may have discontinuous gradients but the viscosity solution remains continuous.

In [6], a method based on singularity-capturing is proposed. We added a couple of ray to figure 16 to obtain figure 17. The viscosity solution is computed first specifying a point source condition (48) at point $x_0 = \mathrm{O}$. The solution gives in particular the travel $t2$ at point I (the earliest travel time, case 1 of section 2). The singularity (thick line) is located by detecting where the gradient of the solution (also given at point $y(s)$ by the slowness vector $p(s)$ of (50) and represented by arrows on the figure) is discontinuous. We also recall tat rays crossing there give the same travel time there (the viscosity solution is continuous).

Then, the trace of the viscosity solution on the kink is used as a source for computing new viscosity solutions on each side of the kink. The remaining part of the rays (dashed line) also realize minima for these new problems with modified source. The new viscosity solution on the upper part of the kink therefore gives travel time $t1$ at point I (case 3 of section 2).

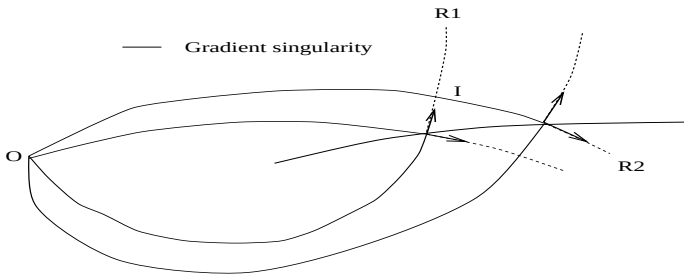

Figure 17:

8.4 A slowness matching algorithm

In this method [29], use is made of the time reversibility of the problem. Integrating the slowness $(1/c)$ along a ray between two points one way or another give the same travel time. Here multi-valuedness is get rid of by splitting the domain using an interface (thick line on figure (18)) and considering point I as source.

First the viscosity solution is computed on the left side of the interface (source point at O). There is a priori no multi-valuedness occurring in this zone so travel times associated to ray R1 and R2 will be computed up to the interface. The idea now is to find the source point on the right side for which the associated viscosity solution will have matching slowness vector (gradient, represented by arrows) with the left side solution at points on the interface.

On figure (18) for instance point I is the correct source. The method will find two slowness matching points (intersection of R1 and R2 with the interface). The viscosity solution associated with a source point at J generates a gradient at the interface discontinuous with the left side gradient at these same points. Note that there is no multi valuedness either on the right side. Rays R1 and R2 have been split such that each part realize a minimum travel time on his side (case 1 section 2). The two different travel-times $t1$ and $t2$ will simply be given by summing the left and right viscosity solutions at these two slowness matching points.

The multi valued solution, on a line of receiver for instance (on the right), is obtained by systematically computing the viscosity solution for a source point on each receiver and then classify the different travel time by slowness matching on the interface.

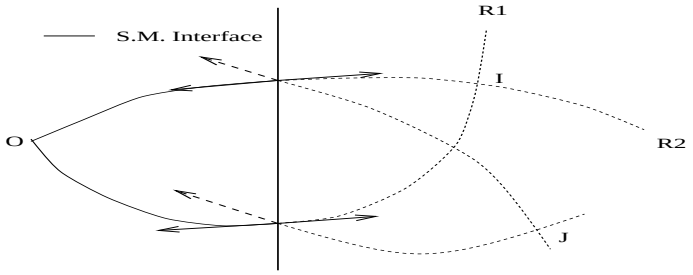

Figure 18:

8.5 Big ray tracing

This method [9] [8] uses the state constrained optimal control characterization of the viscosity solution given in section 2 case 2. The idea is to define local domains, called big rays, using ray tracing such that multi-valuedness will be split between these big rays.

A ray actually realize a stationary point for the Fermat principle. Our idea is to say that every ray realize a local minimum (with respect to the path restricted to lie in its neighborhood). In our particular example we assumed that $t2 < t1$. Ray R2 realize a global minimum for (49) while ray R1 is a local minimum. On figure 19 however, ray R1 will realize a global minimum with respect to to path going from O to I and restricted to lie in the domain BR1 bounded by the thick lines (two rays). Computing the viscosity solution in this domain with boundary conditions as in case 2 of section 2 ($x_0 = \mathrm{O}$) gives $t1$ as ray R1 is a global minimum in BR1 for (49) and exit the domain with zero cost while ray R2 exit with infinite cost.

Based on this idea, the big ray tracing algorithm (as proposed in [9]) simply consist in shooting a sufficient number of ray and systematically compute the viscosity solution between each couple of successive rays. We obtain an approximation of the multi-valued travel time. On figure 20, the thick lines (rays) define a domain BR2 in which, the viscosity

solution gives $t2$. The method gives a multi-valued travel time field in the (non empty) intersection of BR1 and BR2.

It should be noted that in the presence of a caustic, classical geometrical optics cease to be valid and rays do not necessarily realize minima. Special care must be taken and a a treatment based on the geometrical theory of diffraction ([21] [23]). is proposed in [8].

An other approach based on the decomposition of the ray domain (set of initial take-off angles of the rays) into elementary waves [10] is under investigation.

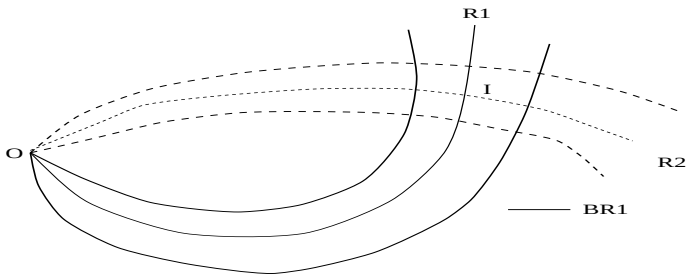

Figure 19:

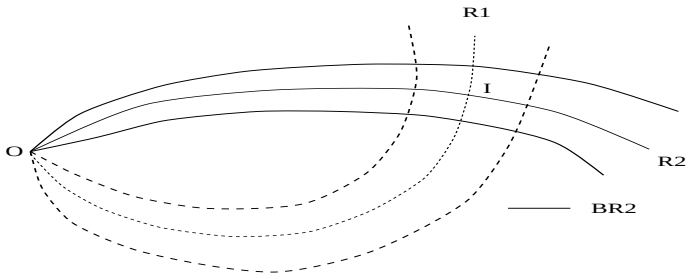

Figure 20:

References

[1] R. Abgrall. Numerical Discretization of First Order Hamilton Jacobi Equations on Triangular Meshes. *To appear in Comm. in Pure and Applied Math.*, 1996.

[2] R. Abgrall. Numerical discretization of boundary conditions for first order hamilton-jacobi equations. *Tech. Report 96031, Universite de Bordeaux 1*, 1997.

[3] R. Abgrall and J.-D. Benamou. Big ray tracing and eikonal solver on unstructured grids : Application to the computation of a multi-valued travel-time field in the marmousi model. *sumitted to Geophysics and INRIA tech. rep. 3019.*

[4] O. Runborg B. Engquist. Multi-phase computation in geometrical optics. *Tech report, Nada KTH*, 1995.

[5] S. Osher B. Engquist, E. Fatemi. Finite difference methods for geometrical optics and related nonlinear pdes approximating the high frequency helmholtz equation. *CAM report 90024-1555, UCLA.*

[6] S. Osher B. Engquist, E. Fatemi. Numerical resolution of the high frequency asymptotic expansion of the scalar wave equation. *J. Comp. Physics*, 120:145–155, 1995.

[7] G. Barles. *Solutions de viscosité des équations de Hamilton-Jacobi.* Springer-Verlag, 1994.

[8] J.-D. Benamou. Big ray tracing : the geometrical theory of diffraction approach. *in preparation.*

[9] J.-D. Benamou. Big ray tracing : Multivalued travel time field computation using viscosity solutions of the eikonal equation. *J. Comp. Physics*, 128:463–474, 1996.

[10] P. Bulant. Two-point ray tracing in 3-d. *PAGEOPH*, 148, 1996.

[11] V. Cerveny. *The application of ray tracing to the numerical modeling of seismic wavefields in complex structures : Handbook of Geophys. Expl.* Geophysical Press, 1985.

[12] C.H. Chapman. Ray theory and its extensions : Wkbj and maslov seismograms. *J. Geophys.*, 58:27–43, 1985.

[13] M. Abd El-magged. 3-d first arrival traveltimes and amplitudes via eikonal and transport finite difference solvers. *Rice University thesis*, 1996.

[14] V. Farra and R. Madariaga. Seismic waveform modelling in heterogeneous media by ray perturbation theory. *J. Geophys. Res.*, 92:2697–2712.

[15] A. Hanyga G. Lambare, P. Lucio. 2-d asymptotic green's functions. In *Proceedings of the 64th SEG annual meeting*, 1994.

[16] P. Gerard, P. Markowich, N.Mauser, and F. Poupaud. Homogenization limits and wigner transforms. *Tech Report, Université de Nice*, 1996.

[17] V. Guillemin and S. Sternberg. Geometric assymptotic. *American Mathematical Society, Providence*, 1979.

[18] A. Hanyga and J. Pajchel. Point to curve ray tracing in complex geological models. *Geophysical Prospecting*, 43:859–872, 1995.

[19] S.V Fomin I.M. Gelfand. *Calculus of Variation.* Prentice-Hall, 1963.

[20] J. B. Keller. Geometrical theory of diffraction. *J. Opt. Soc. Amer.*, 52:116–130, 1962.

[21] J.B. Keller. A geometrical theory of diffraction. In *Calculus of variations and its applications Vol, 8.* McGraw-Hill, New-York, 1958.

[22] P.L. Lions. *Generalized solutions of Hamilton-Jacobi equations.* Pitman, 1982.

[23] D. Ludwig. Uniform asymptotic expansions at a caustic. *Comm. Pure Appl. Math.*, 19:215–250, 1966.

[24] S. Osher and J. Sethian. Front propagating with curvature dependent speed : Algorithm based on hamilton-jacobi formulations. *J. Comp. Physics*, 79:12–49, 1988.

[25] R. Rietdjik. Notes on bigray tracing. In *Shell tech. Report SIEP 97-5105*, 1997.

[26] L. Rudin S. Osher. Rapid convergence of approximate solution to shape-from-shading problem. *Not published (see ref. 26 on this work).*

[27] J. Sethian. Level set methods ... *Acta Numerica*, 1996.

[28] H. M. Soner. Optimal control problems with state space constraints. *SIAM J. Control and optim.*, 24:552–561, 1986.

[29] W. Symes. A slowness matching algorithm for multiple traveltimes. *preprint*, 1996.

[30] W. Symes, R. Versteeg, A. Sei, and Q. H. Tran. Kirchhoff simulation migration and inversion using finite-difference traveltimes and amplitudes. *TRIP tech. Report, Rice U.*, 1994.

[31] E. Rouy. A. Tourin. A viscosity solution approach to shape-from-shading. *SIAM J. Numer. Anal.*, 29:867–884, 1988.

[32] H. M. Soner W. H. Fleming. *Controlled Markov Processes and Viscosity Solutions.* Springer-Verlag, 1993.

[33] L.C. Young. *Lecture on the Calculus of Variation and optimal control theory.* 1969.

Unit´e de recherche INRIA Lorraine, Technopôle de Nancy-Brabois, Campus scientifique,
615 rue du Jardin Botanique, BP 101, 54600 VILLERS LÈS NANCY
Unit´e de recherche INRIA Rennes, Irisa, Campus universitaire de Beaulieu, 35042 RENNES Cedex
Unit´e de recherche INRIA Rhône-Alpes, 655, avenue de l'Europe, 38330 MONTBONNOT ST MARTIN
Unit´e de recherche INRIA Rocquencourt, Domaine de Voluceau, Rocquencourt, BP 105, 78153 LE CHESNAY Cedex
Unit´e de recherche INRIA Sophia-Antipolis, 2004 route des Lucioles, BP 93, 06902 SOPHIA-ANTIPOLIS Cedex

Éditeur
INRIA, Domaine de Voluceau, Rocquencourt, BP 105, 78153 LE CHESNAY Cedex (France)
http://www.inria.fr
ISSN 0249-6399